CEDTECH International Journal of Engineering & Applied Science
Volume 2, Number 1, March 2021
http: / /www.cedtechjournals.org
ISSN: 2756-4533

ELECTRONIC STRUCTURE, OPTICAL AND THERMODYNAMIC PROPERTIES OF GERMANIUM-PHENYL NANOCLUSTER IN THE GAS PHASE: A DFT STUDY.

Njapba S. Augustine[1] and Galandachi M. Garba[2]
[1]Department of Physics, Gombe State University, PMB 127, Gombe State, Nigeria
[2]Department of Physics, Bayero University, Kano PMB 3011, Kano State, Nigeria

ABSTRACT

The molecular geometry of Germanium-phenyl[$Ge_9(C_6H_5)$] nanocluster in the gas phase was studied using ab initio quantum chemical calculation at DFT/B3LYP level of theory employing Lanl2dz basis sets. The most stable molecular structure of germanium-phenyl nanocluster was predicted using the potential energy surface scan of dihedral angle C_{10}-C_9-Ge_{20}-Ge_3 from 0^0 to 360^0 in 10^0 steps with DFT/MP2 method and CEP-31g basis set as implemented in Gaussian 09 program. This molecular structure was optimized and their parameters such as bond lengths, bond angles and dihedral angles were computed at this level of theory. The molecular structure, electronic absorption spectra, thermodynamic properties and vibrational frequencies with IR and Raman intensities have been studied. The calculated molecular geometry revealed no imaginary frequencies, is a tricapped trigonal prismatic distorted planar structure and the Ge-Ge bond distance(2.63-2.98 $\mathring{A}$) and height of 3.126-3.496 $\mathring{A}$ similar with observed experimental values. It is observed that the maximum absorption wavelength(λ_{max}) corresponds in UV spectrum to an intense maximum peak of 658.8 nm with oscillator strength, $(f = 0.0026)$ in the gas phase. This predicted optical absorption wavelength is within the range of visible spectra of about 400-800 nm. The density of State clearly exhibit the possible energy flow from occupied to the virtual states. The calculated emission spectra of germanium-phenyl[$Ge_9(C_6H_5)$] is located in the red visible light region, wavelength(658.9 nm) and energy(1.882 eV).

Keywords: *Germanium, Nanocluster, abinitio, Oscillator Strength, Absorption Wavelength, Geometry Optimization, Potential Energy Surface Scan.*

INTRODUCTION

Germanium and Benzene-like molecular materials have attracted much attention of recent as a post-Silicon technology material with excellent material properties. These materials have potential for a wide range of applications. For instance, Ge like silicon is a semiconductor and its nanocluster have interesting optical and electronic properties. Also, the electronic properties of small organic molecules for technological applications is rapidly growing, thus extended studies for molecule-germanium junctions are needed(Herrera and Seminario, 2007). This work is focused on hybrid germanium-phenyl nanocluster in which their material properties, electronic, optical and thermodynamic properties are studied. The appealing features of hybrid organic-inorganic materials arise from the combination of different properties and functions of the organic phase (low density, high elasticity, good process ability etc.) and the inorganic phase (thermal stability, hardness, high strength, low permeability etc.). Kagan *et al*,(1999) reports that hybrids combines both the superior property characteristics of the crystalline inorganic solids with those of organic molecules within a molecular scaled composite. Moreover, its tuning can obviously generate hybrid materials with properties that are not only the sum of the individual contributions of both phases. Franklin and Steven (2012) reported that hybrid structures that are composed of organic molecules and semiconductor has opened up exciting new areas of development in molecular electronics, nanoscale sensing devices and lithography.

Clayborne and Hakkinen (2012) have reported a systematic density functional theory calculations of the electronic structure of $Ge_9[Si(SiMe_3)_3]_3^-$ cluster, the derivatives revealed that its neutral counterpart have electronic shells. The arrangement of germanium atoms inside the anionic cluster is tricapped trigonal prismatic arrangement which is the usual nine-atom germanium Ge_9 cluster structure. Sun Z.M *et al*.(2009) have also reported the synthesis, experimental and theoretical characterization of $[Ni@(Ge_9PdPPh_3)]^{2-}$. Single point DFT calculation were performed to verify the nature of the clusters on the potential energy surface.

The optimized geometrical parameters were in good agreement with the crystallographic values. Goicoechea and Sevov,(2006) have reported the synthesis, crystal structure characterization and spectroscopic studies of nickel-centered cluster of nine-atom germanium cluster and ligated nickel atom $Ni_2Ge_9[PPh_3]^-$ produced from the reaction of K_4Ge_9 with $Ni(PPh_3)_2CO_3$ in the presence of 2,2,2-crypt(4,7,13,16,21,24-hexaoxo-1,10 diazadicyclo[8,8,8] hexacosane) in ethylenediamine at different temperature(e.g.120^{0}C). Their results revealed a nine-atom germanium Ge_9 cluster core one Ni encapsulated in the centre of the cluster and Ni(PPh_3) fragments capping the cluster. The spectrum also revealed the parent ion as well as all fragments present in the gas phase.

Our focus is on a nine-atom germanium-phenyl[$Ge_9(C_6H_5)$] nanocluster. A bottom-up approach was used to build Germanium-phenyl nanocluster by adding molecules of Germanium and the phenyl ring in order to maintain the stability of the structure. We have applied first principle based DFT calculations with the hybrid functional B3LYP, the MP2 method and LanL2DZ basis sets as implemented in the suit of the software Gaussian 09W to accurately determine all the properties of germanium-phenyl nanocluster. DFT is single particle ***ab initio*** approach that was successfully used to calculate the ground state equilibrium geometry and electronic properties of materials at reduced dimensions. The possibility thereof continue to grow because of the steady increase of calculation capacities but even more due to the continuous development of this very advanced theoretical method. B3LYP exchange correlation functional is known to be well balanced choice in calculations of both molecules and clusters with reliable results. Most popular chosen basis set containing germanium compounds include medium-size LANL2DZ and CEP-31g basis sets. Both basis sets make use of the valence electrons for its calculation. Gaussian 09W is a very popular quantum chemical software program capable of predicting many properties of atoms and molecules utilizing first principle approach. Gauss View is a graphical user interface program designed to simplify and extend the use of Gaussian 09W

program. It incorporates an excellent molecular builder.

Theory

Harmonic Vibrational frequency

From classical mechanics, the kinetic energy of vibration is written as

$$\hat{\mathrm{T}} = \frac{1}{2}\sum_{i=1}^{N} m_i \left[\left(\frac{d\Delta x_i}{dt} \right)^2 + \left(\frac{d\Delta y_i}{dt} \right)^2 + \left(\frac{d\Delta z_i}{dt} \right)^2 \right]$$

(1.1)

where $\Delta x_i, \Delta y_i, \Delta z_i$ are the small displacement between atom i and its equilibrium position X_0. By introducing the mass-weighted Cartesian displacement coordinates q for the 3N degrees of freedom, we have $q_1 = \sqrt{m_1}\Delta x_1, q_2 = \sqrt{m_1}\Delta y_1, q_3 = \sqrt{m_1}\Delta z_1$, and in a more general sense, we defined the locations X_i of the nuclei relative to their equilibrium position X_0 and their masses, m_i as

$$q_i = m_i^{1/2}\left(\mathrm{X}_i - \mathrm{X}_0\right)$$

(1.2)

where the kinetic energy from equation (2.1) becomes

$$\hat{\mathrm{T}} = \frac{1}{2}\sum_{i=1}^{3N} \dot{q}_i^{\,2}$$

(1.3)

The total energy of a molecule is the sum of kinetic energy T, and potential energy, V comprising N atoms near its equilibrium structure may be written as

$$E = T + V = \frac{1}{2}\sum_{i=1}^{3N} \dot{q}_i^{\,2} + V_0 + \sum_{i=1}^{3N}\sum_{j=1}^{3N} \left(\frac{\partial^2 V}{\partial q_i \partial q_j} \right)_0 q_i q_j$$

(1.4)

V_0 is the potential energy at the equilibrium nuclear configuration, and the expansion of the power series is truncated at second order. For such a system, the classical mechanical equation of motion takes the form

$$\frac{d}{dt}\frac{\partial T}{\partial \dot{q}_i} + \frac{\partial V}{\partial q_i} = 0 \quad \text{and}$$

(1.5)

$$\ddot{q}_i = \sum_{i=1}^{3N} f_{ij} q_i, i = 1,2,3 - - - - - 3N$$

(1.6)

The term f_{ij} is mass-weighted quadratic force constant and they are also the elements of the mass-weighted Hessian matrix $\mathbf{H}_{ij}$. i.e.

$$H_{ij} = \frac{\partial^2 E}{\partial q_i \partial q_j}$$

(1.7)

$$f_{ij} = \left(\frac{\partial^2 V}{\partial q_i \partial q_j} \right)_0$$

(1.8)

The mass-weighted Hessian matrix, $\mathbf{H}_{ij}$ is obtained from

$$H_{ij} = \sqrt{m_i} F_{ij} \sqrt{m_j} \quad (1.9)$$

where F_{ij} is the force-constant matrix mass-weighted, the second derivative of the energy with respect to each of the normal coordinates q_i (Leach, 2007), m is a diagonal 3m x 3m matrix that contains the atomic masses. According to the harmonic approximation , the Vibrational frequencies are the square root of the eigenvalues ε_i of F_{ij} and the normal modes are the eigenvectors related to the Vibrational frequency by

$$V_i = \frac{1}{2\pi} \sqrt{\varepsilon_i} \quad (1.10)$$

These vibrational frequencies are used to calculate the infrared (IR) spectrum and Raman spectrum. The intensity of an IR absorption is approximately proportional to the change in the dipole moment with respect to a geometry displacement along a normal coordinate. Similarly, Raman intensities depend upon the derivative of the polarizability with respect to a normal coordinate. Since the polarizability is itself the second derivative of the energy with respect to an applied electric field, the Raman intensity is a third derivative property. Gaussian evaluates Raman intensities analytically.

Thermodynamic Parameters

On the PES, the energies of the various structures whose coordinates are defined by the fixed nuclear positions are determined from quantum mechanical calculations of the electronic energy. This treatment of the energy of motion of the nuclei is linked to molecular vibrations. This is true even at a temperature arbitrarily close to absolute zero, since the lowest Vibrational energy level for any bound vibration is not zero. In the harmonic approximation the zero-point energy is written as

$$E = \frac{1}{2} \sum_{i=1}^{3N-6} h\nu_i \quad (1.11)$$

The frequency calculation from Gaussian also computes the zero-point energy (ZPE) correction, which accounts for the effects of molecular vibrations at 0 K. Statistical mechanics is the bridge between microscopic calculations and thermodynamics of a particle ensemble. The connection between properties of a

microscopic system and a macroscopic sample is provided by statistical mechanics. Thermodynamic correction terms for enthalpy (Hcorr) and entropy (S) were applied to the systems by using the well-known equations for the harmonic oscillator, rigid rotor, and ideal gas from statistical thermodynamics. This was necessary because entropy changes play a huge role in adsorption processes of molecules on surfaces. Accordingly, the Gibbs energy, G, was calculated for all structure using the equations below(Jensen, 2007; Pecher *et al.*, 2017).

$$G = H_{corr} + TS_{corr} \quad (1.12)$$

where

$$H_{corr} = H_{vib} + H_{rot} + H_{trans} \quad (1.13)$$

and

$$S_{corr} = S_{vib} + S_{rot} + S_{trans} \quad (1.14)$$

$$S_{vib} = R\sum_{i=1}^{3N-6}\left[\frac{h\nu_i}{\mathrm{K}_B T}\left(\frac{1}{\exp\left(\frac{h\nu_i}{\mathrm{K}_B T}\right)-1}\right) - In\left(1-\exp\left(\frac{-h\nu_i}{\mathrm{K}_B T}\right)\right)\right]$$

$$S_{rot} = R\left[\frac{3}{2} + In\left(\frac{\sqrt{\pi \mathrm{I}_1\mathrm{I}_2\mathrm{I}_3}}{\sigma}\left[\frac{8\pi^2 \mathrm{K}_B T}{h^2}\right]\right)\right]$$

$$S_{trans} = R\left[\frac{5}{2} + In\left(V\left[\frac{2\pi m \mathrm{K}_B T}{h^2}\right]^{\frac{3}{2}}\right)\right]$$

$$H_{vib} = R\sum_{i=1}^{3N-6}\left[\frac{h\nu_i}{\mathrm{K}_B}\left(\frac{1}{2} + \frac{1}{\exp\left(\frac{-h\nu_i}{\mathrm{K}_B T}\right)-1}\right)\right] \quad (1.15)$$

$$H_{rot} = \frac{3}{2}RT,,,,,H_{trans} = \frac{5}{2}RT \quad (1.16)$$

where N is the number of atoms in a given molecule, R is the gas constant, h is Planck's constant, m is the molecular mass, K_B is the Boltzmann constant, T is the temperature, V is the volume for an ideal gas, $V = {K_B T}/{P}$), σ is the symmetry number for rotation, I

is the moment of inertia, v_i is the Vibrational frequency.

$$C_p = C_{trans} + C_{rot} + C_{vib}$$

$$C_p = \frac{5}{2}R + \frac{3}{2}R + R\sum_{i=1}^{3N-6}\left[\exp\left(\frac{-h\nu_i}{\mathrm{K}_B T}\right)\left(\frac{h\nu_i/\mathrm{K}_B T}{\exp\left(\frac{-h\nu_i}{\mathrm{K}_B T}\right)-1}\right)\right] \quad (1.17)$$

where C_{rot}, C_{vib}, and C_{trans} are contributions to heat capacity due to rotational motion, Vibrational motion and translational motion respectively. These formulas used are only valid at an optimized geometry with respect to all normal coordinates. The frequency calculations also compute zero-point correction which accounts for the effects of molecular vibrations at 0 K.

Computational Details

An a**binitio** and DFT calculations were performed using the Gaussian 09W software package(Frisch *et al*, 2009). We used B3LYP in the DFT calculations. The Basis sets used are Lanl2dz and CEP-31g with the effective core potential by Hay and Wadt(Hay and Wadt, 1985). The PES scan was performed to predict the most stable molecular structure of the nanostructure using B3LYP/CEP-31G basis set. The most stable molecular structure

The heat capacity at constant pressure, Cp is given by the equation

was optimized at DFT/ MP2 and DFT/B3LYP methods with Lanl2dz basis set using Gaussian 09 program in the framework of unrestricted formalism. Harmonic vibrational frequencies were computed at the same level in order to characterize the structure. The predicted harmonic frequencies are not scaled in the current study. The optimized structural parameters of $[Ge_9(C_6H_5)]$ nanocluster were used to characterize all stationary points as minima. To study the vibrational nature of the nanocluster, the IR and Raman spectra of $[Ge_9(C_6H_5)]$ were calculated by taking the second derivative of the energy that is computed analytically and compared. The excitation energies and the corresponding UV-Vis spectra of germanium-phenyl$[Ge_9(C_6H_5)]$ nanocluster were calculated using time-dependent density functional theory method (TD-DFT)with CAM-B3LYP basis sets based on the ground state structure. Gauss Sum 3.0(O^1Boyle *et al*, 2008) was

used to determine HOMO-LUMO energy gap and density of state (DOS) spectrum of germanium-phenyl[$Ge_9(C_6H_5)$] nanostructure. In order to check the validity of the applied methodologies, a trial calculation is carried out on Ge-Ge dimer. Calculated Ge-Ge bond length is 2.64Å
which is within the range of the values obtained theoretically as well as experimentally reported by Clayborne and Hakkmen,(2012). The correlation between the statistical thermodynamics and temperature were also obtained. It is observed that the heat capacity, enthalpy and entropy increase with the increasing temperature owing to the fact that the intensities of the molecular vibrations increase with temperature.

RESULTS AND DISCUSSION

Potential Energy Surface (PES) Scan.

The nine-atom germanium-phenyl[$Ge_9(C_6H_5)$] cluster in the gas phase, was built by using Gaussian 09W software package(See **Figure 2 below**, a rigid PES scan was performed to predict the most stable molecular structure using DFT/B3LYP method with CEP-31g basis sets. The conformational space arrangement of the nanocluster was investigated by running its PES scan through the rotation of C_{10}-C_9-Ge_{20}-Ge_3 torsion angle at the Ge_{20} atom with a step size of 10^0 in the range of 0^0 to 360^0 with all other geometrical parameters kept fixed. However, relatively small step size are needed so that energy and angular momentum are conserved with sufficient accuracy. All calculations were carried out using my personal computer without any constrain on the geometry. In principle, the conformational space of a system can be explore by rotating all the internal rotational degrees of freedom. Different combinations of the rotational bonds will give rise to an individual conformer which has its own electronic energy and correspond to one point on the PES.

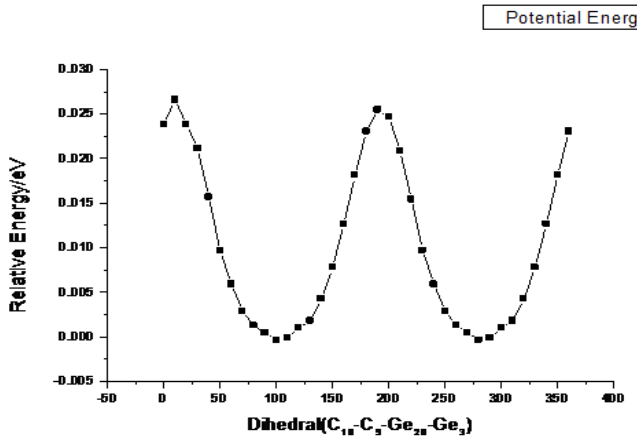

Figure 2: PES scan curve of Germanium-phenyl[$Ge_9(C_6H_5)$] nanocluster along dihedral C_{10}-C_9-Ge_{20}-Ge_3 at B3LYP/CEP-31g basis set.

After convergence, the scan plot of the relative energies and the angle of rotation with respect to the dihedral angle derived from PES scan is shown in **Figure 2.** The PES scan revealed 37 conformers. There are minima and maxima on the PES representing different conformers and isomers of the nanocluster. For a point on the PES to be a minimum, it must satisfy the following conditions: first derivative of the energy with respect to the nuclei position must be zero(i.e. stationary point). If it is not zero then there is a nearby point that is lower in energy. The second derivative of the energy with respect to the nuclei coordinates must be positive. In other words, all eigenvalues of the Hessian must be positive for a minimum or all the vibration frequencies must be real(i.e. no imaginary frequencies). The Figure shows three maxima at 20^0, 200^0 and 360^0 with corresponding maximum energies of 30 , 26.3 and 22.5 meV respectively. The two minima having most stable conformation are found at 100^0 and 280^0 with relative energy of 0 eV for C_{10}-C_9-Ge_{20}-Ge_3 torsional angle . The PES scan thus indicates that the Germanium-phenyl[$Ge_9(C_6H_5)$] nanocluster is most stable at 100^0 with respect to [C_{10}-C_9-Ge_{20}-Ge_3] dihedral angle rotation. At this point on the PES the equilibrium geometry structure parameters are in their ground state.

According to Boltzmann theory, only a few local stable structure with low electronic energies on the PES may dominate the conformational distribution and are responsible for measured

properties. The probability that a molecule would take on a conformation with energy ΔE_i is given by the Boltzmann distribution:

$$\frac{N_i}{N} = \frac{\exp\left[\frac{-\Delta \mathrm{E}_i}{\mathrm{K}_B T}\right]}{\sum_i \exp\left[\frac{-\Delta \mathrm{E}_i}{\mathrm{K}_B T}\right]}$$

(1.18)

where ΔE_i is the relative energy of the i[th] conformer with respect to the lowest energy, K_B is the Boltzmann constant($K = 1.38 \times 10^{-23} J / K$), and the temperature is set at 298 K, the summation runs over the number of possible conformers. As it is possible that a number of different states (conformers or local minima) will be thermally populated at a given finite temperature, the corresponding Boltzmann population analyses based on the relative energies were performed using equation(4.1) at B3LYP/CEP-31g. From **Table 1**, the highly populated stable molecular geometry (i.e. percentage of occupation, 34) has the least relative energy of 0 meV with dihedral angles of 100^0 and 280^0 respectively. Also the highest energy(30.0 eV) is the least populated(16.4).

Table 1: Conformation analysis of [$Ge_9(C_6H_5)$] at B3LYP/CEP-31g basis set.

Dihedral (C_{10}-C_9-Ge_{20}-Ge_3)	**Number of conformers**	ΔE_i **/meV**	**N/%**
0	1	23.8	19.2
20	2	30.0	16.4
30	3	24.0	18.9
40	4	21.3	20.3
50	5	16.3	22.9
55	6	10.0	26.7
60	7	6.3	29.2
70	8	2.5	32.0
80	9	1.3	33.0
90	10	0.63	34.0
100	11	0.0	34.0
110	12	0.31	34.0
125	13	3.8	31.0
135	14	2.5	32.0
140	15	5.0	30.1
150	16	8.8	27.5

160	17	15.0	23.6
175	18	20.0	20.9
190	19	25.0	18.5
200	20	26.3	17.9
210	21	25.0	18.5
225	22	21.3	20.2
235	23	16.3	22.9
245	24	10.0	26.7
250	25	6.3	29.2
260	26	2.5	32.0
265	27	1.3	32.9
270	28	0.63	33.5
280	29	0.0	34.0
290	30	0.42	33.7
300	31	1.25	33.0
315	32	2.5	32.0
325	33	5.0	30.1
335	34	7.5	28.3
350	35	12.5	29.6
355	36	17.5	22.2
360	37	22.5	19.7

Geometry Optimization and Molecular Structure

The first step in our study was the PES scan of nine-atom Germanium-phenyl [$Ge_9(C_6H_5)$] nanocluster to determine the most stable equilibrium structure. This was done using DFT/B3LYP functional and CEP-31g as the basis set. The obtained molecular structure is used as input for the geometry optimization. This is the most common calculation performed in many computational programs to optimized the molecular structure to a minimum on the potential energy surface Full geometry optimization was performed for the structure using a gradient minimization technique, to find the stable atomic arrangement of the structure. All the minima were characterized by having zero gradient norms and by diagonalizing the matrix of the second derivatives to give positive harmonic vibrational frequencies . Once optimized, frequency calculations were carried out using the same functional and basis set . Density functional theory calculations with Moller-Plesset perturbation theory(MP2) at LANL2DZ basis set using the

Berny algorithms were performed with Gaussian 09W and Gauss View software package(Foresman and Frisch, 1996; Frisch *et al*., 2009). The nine-atom germanium- phenyl [$Ge_9(C_6H_5)$] nanocluster was fully optimized. All calculations were performed using my personal computer without any constrain on the geometry. After convergence, the nanocluster has C_1 point group symmetry the bond length, bond angles and dihedral angles of the nanocluster are characteristic properties of a material. Since the molecules are always in a state of vibration, these values are dependent on the method measurements(Suna *et al*.,2016). **Figure 3** below shows the optimized molecular structure of Germanium-phenyl[$Ge_9(C_6H_5)$] nanocluster with atomic numbering scheme. The geometric optimized parameters of the cluster calculated at DFT/MP2 levels with Lanl2dz basis set are listed in **Table 2**.

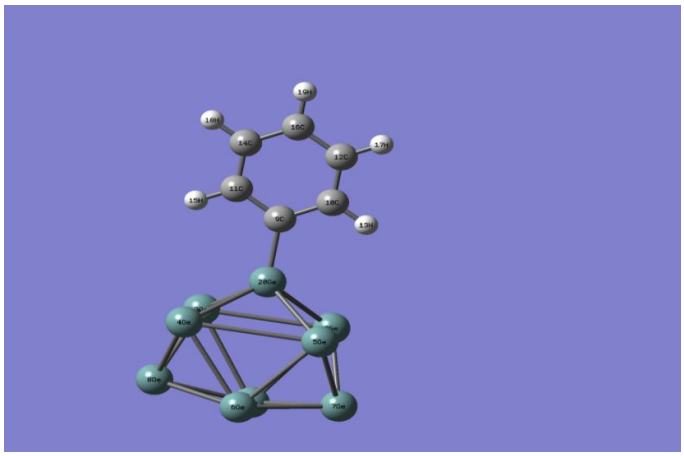

Figure 3: Molecular Structure and atomic numbering with use of ,Germanium-phenyl [$Ge_9(C_6H_5)$] nanocluster.

From **Figure** 3, the arrangement of the nine-atom germanium inside the cluster compound is viewed as a tricapped trigonal prismatic arrangement with the triangular base made up of atoms 1-7-8 and 6-7-8, the bulky phenyl group capped the cluster. The nine-atom germanium cluster is a cage and has distorted geometrical structure. This structure agrees with similar molecular structures reported in literature(Goicoechea and Sevov,2006; Hansen *et al*.,2012; Pancharatna and

Hoffmann,2006). Examining the molecular structure, the Ge-Ge bond distance in the cluster is in the range of 2.635-2.984 Å with edge elongations observed at 3.126, 3.128, 3.353 and 3.496 Å with respect to the bond distances in the element structure. The bond distance of 3.496 Å is in the range of Ge-Ge single bond and thus very long for a germanium atom with coordination number nine. The experimental value of Ge-Ge bond distance is about 2.58 Å. The bond distance reported here compares very well with other similar observed structure $[Ge_9[Si(SiMe_3)]]$ of about 2.63 Å (Clayborne and Hakkmen, 2012).

Table 2: The optimized geometric parameters for Germanium-phenyl$[Ge_9(C_6H_5)]$ atMP2/LanI2dz basis set with bond length (Å), bond angles and dihedral angles in degrees.

Bond	**Bond length (Å)**	**Bond**	**Bond angle/degree**	**Dihedral**	**Calculated bond angles/degree**
Ge1-Ge2	3.128	Ge2-Ge1-Ge6	83.088	Ge6-Ge1-Ge2-Ge5	3.86
Ge1-Ge3	3.128	Ge2-Ge1-Ge8	105.44	Ge8-Ge1-Ge2-Ge20	0.132
Ge1-Ge6	2.959	Ge3-Ge1-Ge7	105.40	Ge3-Ge1-Ge6-Ge4	3.88
Ge1-Ge7	2.879	Ge7-Ge1-Ge8	111.15	Ge3-Ge2-Ge5-Ge4	0.0009
Ge1-Ge8	2.879	Ge1-Ge2-Ge5	93.48	Ge20-Ge4-Ge6-Ge7	0.96
Ge2-Ge3	3.353	Ge1-Ge2-Ge20	97.06	Ge2-Ge5-Ge6-Ge1	4.09
Ge2-Ge5	2.983	Ge3-Ge2-Ge5	91.33	Ge20-C9-C11-C15	0.32
Ge2-Ge7	2.635	Ge3-Ge2-Ge7	105.32	C9-C10-C12-C16	0.054
Ge2-Ge20	2.637	Ge7-Ge2-Ge20	106.37	C9-C11-C14-C16	0.015
Ge3-Ge4	2.984	Ge1-Ge3-Ge4	93.52	C11-C14-C16-C12	0.01
Ge3-Ge8	2.634	Ge1-Ge3-Ge20	97.08	H13-C10-C12-H17	0.12
Ge3-Ge20	2.636	Ge2-Ge3-Ge4	92.42	C9-C11-C14-H18	179.98
Ge4-Ge5	3.496	Ge2-Ge3-Ge8	105.40	H15-C11-C14-C16	180.00
Ge4-Ge6	2.959	Ge8-Ge3-Ge20	106.46	H17-C12-C16-H19	0.16
Ge4-Ge8	2.727	Ge3-Ge4-Ge5	88.58	C11-C14-C16-H19	179.81
Ge4-Ge20	2.663	Ge3-Ge4-Ge6	85.58	H18-C14-C16-C12	180.03
Ge5-Ge6	2.960	Ge5-Ge4-Ge8	103.27	Ge6-Ge1-Ge3-Ge4	-3.82
Ge5-Ge7	2.725	Ge6-Ge4-Ge20	89.42	Ge7-Ge1-Ge3-Ge20	-0.06
Ge5-Ge20	2.661	Ge8-Ge4-Ge20	103.13	Ge2-Ge1-Ge6-Ge5	-3.92
Ge6-Ge7	2.771	Ge2-Ge5-Ge4	88.67	Ge3-Ge1-Ge7Ge5	19.29
Ge6-Ge8	2.769	Ge2-Ge5-Ge6	85.62	Ge2-Ge1-Ge8-Ge4	-19.38
C9-Ge20	1.965	Ge4-Ge5-Ge7	103.29	Ge5-Ge2-Ge3-Ge4	-0.001
C9-C10	1.435	Ge6-Ge5-Ge20	89.42	Ge7-Ge2-Ge3-Ge8	-0.06

C9-C11	1.435	Ge7-Ge5-Ge20	103.19	Ge1-Ge2-Ge5-Ge6	-3.85
C10-C12	1.425	Ge1-Ge6-Ge4	97.62	Ge1-Ge2-Ge20-C9	-155.33
C11-C14	1.425	Ge1-Ge6-Ge5	97.54	Ge1-Ge3-Ge20-Ge9	155.25
C12-C16	1.426	Ge4-Ge6-Ge7	117.60	Ge3-Ge4-Ge5-Ge2	-0.001
C14-C16	1.426	Ge5-Ge6-Ge8	117.60	Ge8-Ge4-Ge5-Ge7	-0.058
C10-H13	1.096	Ge7-Ge6-Ge8	117.97	Ge3-Ge4-Ge6-Ge1	-4.06
C11-H15	1.096	Ge1-Ge7-Ge5	105.20	Ge5-Ge4-Ge8-Ge1	-19.49
C12-H17	1.095	Ge2-Ge7-Ge6	96.67	Ge6-Ge4-Ge20-C9	-161.91
C14-H18	1.095	Ge1-Ge8-Ge4	105.19	Ge8-Ge4-Ge20-C9	-141.07
C16-H19	1.095	Ge3-Ge8-Ge6	96.63	Ge20-Ge5-Ge6-Ge8	-0.88
		Ge2-Ge20-Ge4	118.00	Ge6-Ge5-Ge20-C9	161.92
		Ge3-Ge20-Ge5	117.97	Ge7-Ge5-Ge20-C9	-141.05
		Ge3-Ge20-C9	120.18	Ge4-Ge6-Ge7-Ge2	-20.33
		Ge4-Ge20-C9	121.81	C11-C9-C10-C12	-0.03
		Ge5-Ge20-C9	121.77	Ge20-C9-C10-C13	-0.41
		Ge2-Ge20-C9	120.11	C10-C9-C11-C14	-0.01
		C10-C9-Ge20	120.49	C10-C9-C11-C15	-179.99
		C11-C9-Ge20	120.47	Ge20-C9-C11-C14	-179.69
		C9-C10-C12	120.35	Ge20-C9-C11-C15	0.32
		C9-C11-C14	120.38	C10-C9-Ge20-Ge3	-132.76
		C10-C12-C16	120.19	C10-C9-Ge20-Ge4	145.13
		C11-C14-16	120.17	C11-C9-Ge20-Ge2	141.58
		C12-C16-C14	119.87	C9-C10-C12-H17	-179.96
		C10-C9-C11	119.03	H15-C11-C14-H18	-0.046
		C9-C10-H13	120.35	C10-C12-C16-C14	-0.05
		C12-C10-H13	119.29	C10-C12-C16-H19	-179.85
		C9-C11-H15	120.33	H17-C12-C16-C14	-180.04
		C14-C11-H15	119.29	H18-C14-C16-H19	-0.15
		C10-C12-H17	119.73		
		C16-C12-H17	120.08		
		C11-C14-H18	119.74		
		C16-C14-H18	120.09		
		C12-C16-H19	120.06		
		C14-C16-H19	120.07		

However, we find that the relaxed structure has slightly longer bond length than what is obtained experimentally. As observed, the nine-atom germanium-phenyl structure suffers from intense disorder, apparently adopt the shape of a strongly distorted tricapped trigonal prism with unequal elongated prisms height in the range of 3.128-3.496 Å. Overall, the bond distances within the nine-atom germanium cluster are very similar to the known monosubstituted clusters such as $[Ge_9\text{-}Ge_9]^{6-}$ and $[Ge_9\text{-}SnMe_3]^{3-}$ (Hull and Sevov, 2009) .

The Ge-C bond distance is about 1.965 Å. Hull and Sevov,(2009) reports that the Ge-

C bond distance in the main cluster [Ge_9---C(Me) = CH-CH_2CH_3]$^{3-}$ is about 2.04 Å. Although the precision of our calculated bond distance is lower due to disorder, this is within the range of a Ge-C bond distance[1.82-2,05 Å] according to the Cambridge structural data base(Allen, 2002). The phenyl ring is a regular hexagon with C=C bond distance somewhere between the normal bond distance of 1.54 Å and a double bond distance of 1.33 Å i.e. about 1.44 Å which is equivalent to the value obtained from x-ray diffraction data(Elmali *et al*.,1999). This usual behavior of benzene is due to the strong conjugational effect. The C=C bond distance has not deviated significantly from typical value of 1.339 Å. The C-H bond distance within the phenyl ring on average is about 1.095 Å. Experimentally, the C-H bond length is 1.094 Å(Sholl and Steckel, 2009). Theoretical calculations with Gaussian 09W is expected to be superior to x-ray diffraction method of computing location of hydrogen because the scattered intensity which is proportional to the atomic number is expected to be least for this atom(Reena *et al*.,2013).

Within the nine-atom germanium cluster core, the clusters are arranged in a nearly perfect cube as many of the Ge-Ge-Ge bond angles fall in the range 90 ± 3^0, with some of the angles less than right angles. Similarly, some of the bond angles within the cluster core and the phenyl ring are in the range 105.44-121^0 typically larger than normal tetrahedral angles. This disparity arises due to the presence of the bulky phenyl ring. However, the structure is observed to be planar with bond angles in the range of 115.44-121.81^0 .The deviation of bond angles from 120^0 shows increase of non-planarity of the cluster. Planarity of a molecule can be also confirmed from their dihedral angles. Generally, dihedral angle values of 0^0, 180^0, or 360^0 show planarity of the molecules (Suna *et al*.,2016). Ge-Ge-Ge-Ge dihedral angles with values of 0.132, 0.96, 161.92, 179.664, 179.891, 180.05 degrees indicate in-plane from Ge_{20}-C_9 and nearly planar structure while the dihedral angles with values of -179.69, -179.96, -179.99, 179.89 degrees indicate a slight distortion of planarity from Ge_{20}-C_9.Thus, the bond angle analysis envisage a planar geometry.

Harmonic Vibrational Frequency

Vibrational frequencies are computed by determining the second derivatives of the energy with respect to the Cartesian nuclear coordinates, and then transforming to mass-weighted coordinates. These vibrational frequencies are used to calculate the infrared (IR) spectrum Raman spectrum as shown in **Figure.4(a)** and **4(b)**. **Figure. 4 (a)** and **4(b)** show the IR spectrum and Raman spectrum respectively.

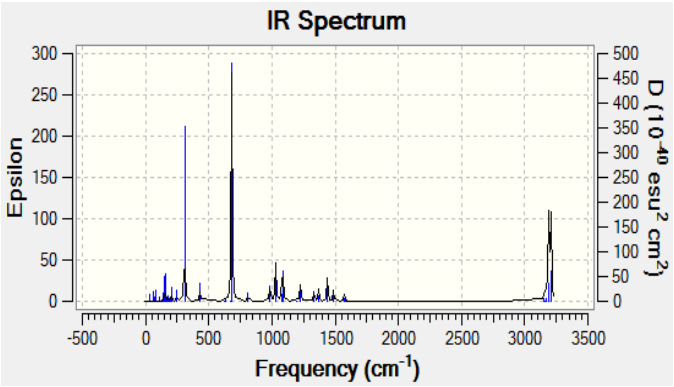

Figure 4(a): IR Spectra of germanium-phenyl nanocluster in gas phase

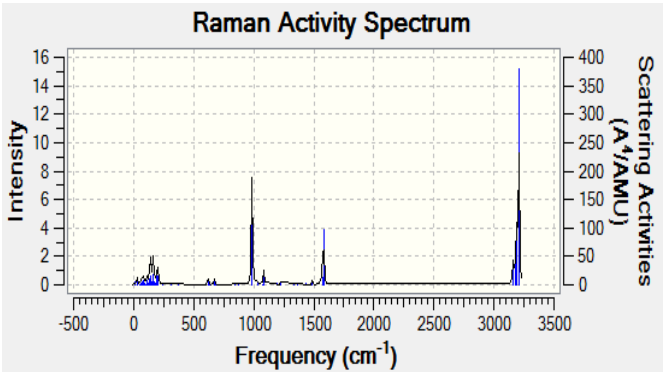

Figure 4(b): Raman Spectra of germanium-phenyl nanocluster in gas.

Germanium-phenyl[$Ge_9(C_6H_5)$] nanocluster has 20 atoms, C_1 symmetry thus, 54 normal modes of vibration. Both IR and Raman spectra fall in the range of 0 to 3500 cm^{-1} respectively. As expected some modes observed in Raman are not observed in the IR spectra and vice versa. In the spectral range 1581-3156 cm^{-1} no bands are available, while some calculated modes have corresponding values in both spectra's. However, the crystal

has inversion center, so the Raman active modes are not active in the IR . Careful observation shows the presence of mainly three to four dominating modes in IR and Raman spectra for the cluster. A lower number of Vibrational modes in IR are basically the indication of the vibration of the bonds(stretching) present in the structure nearly at the same frequency or within a very narrow frequency range. This is because of the strong structural symmetry of the cluster. This lower vibration frequency modes in IR appear at 30.95, 79.21, 147.56, 159.53, 170.77, 206.18, 308.82 cm^{-1} are assigned germanium cluster stretching modes. Raman frequency in general indicates the bending mode in the cluster. The dominating higher mode frequency with very high intensity is the stretching mode of the cluster atoms ,while the IR intensities have about four peaks corresponding to the motion of C-H cluster atoms in different directions.

In the region between 30 to 600 cm^{-1}, we observed an intense band at 308.82cm^{-1}. Frequencies in the range of 206.18-56.15 cm^{-1} are related to Ge-Ge stretching vibrations(breathing modes). As mentioned previously, this frequency region that is less than 308.82 cm^{-1} is due mainly to the vibration of germanium cluster, it is cage an indication of the heaviness of germanium element. Strong vibration peaks appear at 308.82, 682.28, 3206.24 cm^{-1}. No experimental results is available for comparism.

The region between 600 to 1600 cm^{-1}, we observed the various vibration modes of the phenyl ring while the germanium cluster atoms remain static. Also within these region, we have intense peaks at 682.28 cm^{-1} for IR spectra and about 986 cm^{-1} for the Raman spectra that is associated with symmetric stretching mode of vibration. The ring stretching vibrations play a vital role in aromatic systems. The conjugated carbon atoms in the aromatic system undergo coupled vibrations called skeletal vibrations(Suna *et al*,2016). The semicircle stretching of carbon atoms in the aromatic system is due to conjugated double and single bonds lie in between 1487-1580.79 cm^{-1}.

The region between 1600-3220 cm^{-1}, the Raman and IR showed no bands. This was expected since the units forming the cluster have no vibration with energy in this region. The phenyl ring spectral region predominantly involves the C-H, C-C and C=C stretching and C-C-C as well as

H-C-C bending vibrations. The ring stretching vibrations are very prominent in the vibration spectra of Benzene and its derivatives. Usually the carbon hydrogen stretching vibrations give rise to bands in the region of 3100-3000 cm^{-1}in all aromatic compounds(Suna *et al*, 2016). In this present study, the bands in the region 3156.04 3158.39, 3174.65,and 3206.24 cm^{-1} have been assigned to the ring C-H stretching vibrations. In this region also the bands are not appreciably affected by the germanium cluster. Generally, the C-H stretching vibration occur in the region of 2975-2850 cm^{-1} for aliphatic hydrocarbons but this value increases for strained ring system(Raj *et al*.,2017). This high frequency region indicates higher bond energy between the elements. The C-H in-plane and out-of-plane bending vibration generally lies in the range 1300-1000 cm^{-1} and 1000-675 cm^{-1}(Reena *et al*, 2013) respectively. In this work, vibrations involving C-H in-plane bending are found in the region 1487.47-1029.15 cm^{-1} while bending modes less than 1000 cm^{-1} correspond to out-of-plane mode

Table 3 Calculated Vibrational frequency, IR and Raman values of $[Ge_9(C_6H_5)]$ at DFT/MP2 level using LANL2DZ as basis set.

Frequency/cm	IR	Raman	Frequency /cm	IR	Raman	Frequency /cm	IR	Raman
14.69	0.0001	4.6150	145.09	0.0146	6.7024	431.26	3.8023	0.1887
30.26	0.0009	1.3361	147.56	1.8924	4.4409	621.37	0.1008	6.7188
30.96	0.01055	5.1188	159.53	2.2246	5.5586	631.33	0.5583	0.0510
56.15	0.0042	1.2346	161.13	0.9216	18.9399	670.40	0.1846	8.1165
64.61	0.3270	3.1171	170.77	0.3474	6.1366	682.28	82.4073	0.6789
75.68	0.1612	3.8913	172.97	0.1876	0.2880	781.08	0.0210	0.0347
79.21	0.4375	7.1686	178.97	0.4367	2.0530	812.29	3.1573	0.4672
87.72	0.0065	2.6779	188.17	0.2900	4.9355	844.16	0.0016	0.0270
99.30	0.0050	0.2082	195.81	0.3531	14.1350	876.74	0.1256	0.0200
107.39	0.0631	7.9612	204.84	0.2902	15.6912	985.72	7.8465	146.7793
111.39	0.2579	5.0465	206.18	1.3903	1.7392	1029.15	14.5850	2.3207
125.30	0.0120	2.7788	146.37	1.3536	1.6875	1075.27	3.5805	0.2357
133.49	0.0052	10.8005	308.82	27.2705	0.4734	1084.44	16.7774	16.4901
142.31	0.5621	16.3498	376.43	0.0008	0.5824	1198.19	0.0958	3.3337
						1226.95	8.6420	5.2258
						1334.54	6.1369	0.0075
						1369.45	4.1727	3.6680
						1439.59	11.4440	2.9478
						1487.47	4.9688	6.1503
						1572.67	2.1643	12.2143
						1580.79	0.7489	96.2974
						3156.04	4.3981	1.9177
						3158.39	0.3233	37.7614
						3174.65	4.6506	55.2520
						3189.21	29.9160	90.8322
						3206.24	493422	379.0577

To further validate our methodology herewith MP2 level at LANL2DZ basis set, harmonic vibration frequency calculations at specific bond length of the nanocluster were determined. Detailed results are presented in **Table 4.** We obtained 2.66 Å bond length and stretching mode frequency 207 cm^{-1} for Ge-Ge bond distance in the ground state which is reasonably close to the reported values of 2.409 Å and 277 cm^{-1}, 2.44 Å (with lowest value of 250 cm^{-1}) [Wielgus *et al*, 2008; Kapil *et al*.,2012]. The bond length and vibration frequency of Ge-C in the ground state are 1.97 Å and 986 cm^{-1} respectively. Goswami *et al*., (2015) reports Ge-C bond length of 1.80 Å and stretching mode frequency 812 cm^{-1}, is lower than the calculated

value and a similarly high frequency of 943 cm^{-1} has been obtained by Shim *et al*., (1998). IR and Raman activities show distinct spectra for the nanocluster and it reflects the effect of structural change and bonding nature. This is helpful to identify the ground state structure in experiments where necessary(Atobe *et al*., 2012), Detailed frequency analysis is shown in **Table 3**.

Table 4 Selected Bond length and Lowest Frequency of Ge-Ge, Ge-C, C=C and C-H bonds respectively

Interatomic bond	Bond Length ($\mathring{A}$)	Lowest Frequency/cm
Ge-Ge	2.63, 2.66(2), 2.77, 2.87, 2.96	205, 207, 171,141, 111
Ge-C	1.97, 1.97, 1.97, 1.95	6.90, 986, 1027, 1084
C=C	1.43(3), 1.44(2)	682, 986, 1029, 1369
C-H	1.095(2), 1.096(2)	781, 812,844,1227

Prediction of Thermodynamic Properties

The predicted harmonic frequencies are not scaled in the current study. From the vibrational frequency calculation run at B3LYP/Lanl2dz and MP2 levels the values of some thermodynamic parameters(such as zero point vibrational energy, dipole moment, correction energies, rotational temperature and rotational constant) at standard temperature 298.15 K and 1.00 Atm pressure along with the standard statistical thermodynamic functions: standard heat capacities (C_p), standard entropies (S), and standard enthalpy (H) were obtained and results listed in **Table 5.** It can be found from **Table 5** that the zero-point vibration energies were observed to be higher in B3LYP method than MP2. An identical pattern was observed while recording rotational constants, dipole moment, specific heat at constant volume and thermal energy. The zero-point energy(minimum energy due to uncertainty principle) is a correction of the electronic energy to account for the effects of molecular vibrations that persist at 0 K. The disparity in this results could be because the two methods have different approximations in their approach as well as MP2 is wave function based while B3LYP is density function based. On the other hand, specific heat values were found to be lower in B3LYP than inMP2 method. This represent its capability to contain heat. At this low enough value of temperature, 298.15 K

only Vibrational component of the total energy contributes being higher in MP2 than in B3LYP while the translational and rotational components at both levels of the theory remain constant. The dipole moment which gives the molecular charge distribution, was studied to depict the charge moment across the nanocluster. Thus, it is observed that the nanocluster has a dipole moment higher in B3LYP/LANL2DZ than in MP2/LANL2DZ. Entropy is a measure of molecular disorder and is significantly affected by temperature. At this temperature, 298.15 K, only Vibrational and electronic components of the motion contribute to the total entropy with higher values at B3LYP/LANL2DZ[95.027 Cal/mol K] and lower values at MP2[92.093Cal/mol K] while translational and rotational energies remain unchanged. There is a similar trend for thermal energy with the Vibrational component being greater at B3LYP than at MP2. Similarly , it is observed that dipole moment, E, E1, E2, E3, and E4, vary slightly using MP2 and B3LYP levels of theory.

Table 5: Calculated thermodynamic parameters of nine-atom Germanium-phenyl $Ge_9(C_6H_5)$] nanocluster in ground-state at 298.25 K.

Basis set	**MP2**	**B3LYP**
	LANL2DZ	**LANL2DZ**
Zero point Vib energy(J/mol)	59.53	61.02
SCF energy(a,u)	-263.746	--265.575
Rotational Constant(GHZ)		
A	0.18225	0.18148
B	0.11182	0.11257
C	0.09477	0.09539
Specific heat(C_v)[Cal/mol K]		
Total	68.665	67.393
Translation energy	2.981	2.981
Rotation energy	2.981	2.981
Vibration energy	62.703	61.431
Dipole Moment (Debye)	3.5420	3.5836
Entropy(S)[Cal/mol K]		
Total	175.527	178.452
Electronic	0	1.377
Translation	45.693	45.693
Rotation	36.363	36.354
Vibration	92.093	95.027
Thermal energy[KCal/mol]		
Total	73.863	75.337

Translation	0.889	0.889
Rotation	0.889	0.889
Vibration	72.035	73.559
E	-263.746	-265.575
E1	-263.628	-265.482
E2	-263.629	-265.459
E3	-263.628	-265.458
E4	-263.711	-265.543

E=Electronic energy without ZPE corrections, E1=Electronic energy plus ZPE corrections, E2= Electronic energy plus thermal energy plus scaled ZPE, E3= Electronic energy plus enthalpies without unscaled ZPE, E4= Gibbs energy plus without unscaled ZPE. Based on the vibrational analysis at B3LYP/Lanl2dz level and statistical thermodynamics, the standard thermodynamic functions, heat Capacity($C_{p,m}^{0}$), entropy(S_{m}^{0}), and enthalpy($\Delta \mathrm{H}_{m}^{0}$) were calculated in the temperature range 100-1000 K and results are listed in **Table 6**. The variation of the thermodynamical quantities with temperature is shown in **Figure 5**.

Table 6: The Thermodynamic Properties of Germanium-Phenyl nanostructure at Different Temperatures at B3LYP/Lanl2dz level.

T(K)	$\Delta \mathrm{H}_{m}^{0}(\mathrm{K} Jmol^{-1})$	$C_{p,m}^{0}(Jmol^{-1}\mathrm{K}^{-1})$	$S_{m}^{0}(Jmol^{-1}\mathrm{K}^{-1})$
100.00	11.51	192.97	479.53
200.00	33.89	247.27	638.43
300.00	60.42	282.78	748.94
400.00	90.27	313.68	837.04
500.00	122.93	339.05	911.72
600.00	157.85	359.14	976.89
700.00	194.57	375.09	1034.79
800.00	232.71	388.07	1086.87
900.00	272.06	398.79	1134.19
1000.00	312.38	407.75	1177.56

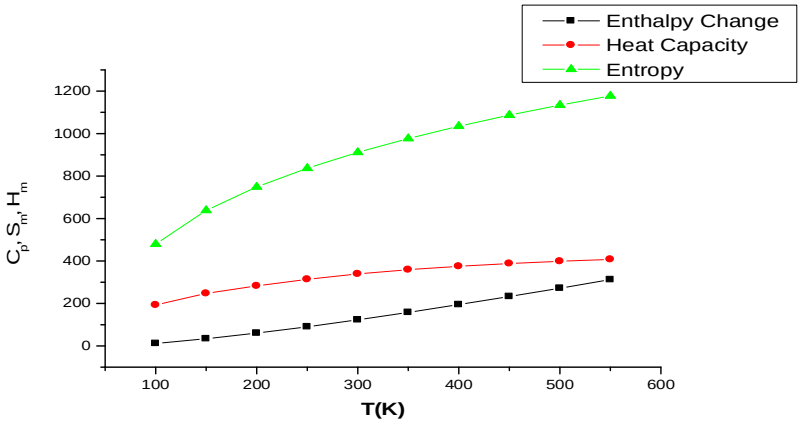

Figure 5: Correlation graphs of Heat Capacity, Entropy, and Enthalpy change Calculated at various Temperatures.

As observed from **Table 5** and **Figure 5**, the standard heat capacity, entropy and enthalpy change increase at any temperature from 100 K to 1000 K, with great increase for entropy and least for enthalpy change, due to the fact that the intensities of molecular vibration increase as the temperature increases.

Optical Properties

The optical properties of an optimized nine-atom germanium-phenyl[$Ge_9(C_6H_5)$] nanocluster were calculated using the time-dependent density functional theory(TD-DFT) which has been successfully applied to study the lowest excitation states and absorption spectra of nanomaterials (Saikia *et al*., 2016). We simulated the absorption spectra using the TD-DFT method as implemented in the Gaussian 09W package. The TD-DFT calculations were implemented using CAM-B3LYP level and LANL2DZ basis set for the nanocluster. A total of ten lowest-energy singlet excited states were considered to account for the major excitations in the UV-visible range. Simulated results calculated using TD-DFT at CAM-B3LYP/LANL2DZ basis set was converted to Gaussian functions using GaussSum 3.0 software (O'Boyle *et al*., 2008) to convolute the energy of the transitions. To represent realistic looking spectra the full width at half maximum of the Gaussian function was set at 3000 cm^{-1}. GaussSum uses Gaussian curves to convolute the electronic transitions and energy levels. The

absorption wavelength, excitation energies, oscillator strength presented in **Table 6.** The **Figure 6** shows the recorded and simulated UV-vis spectra

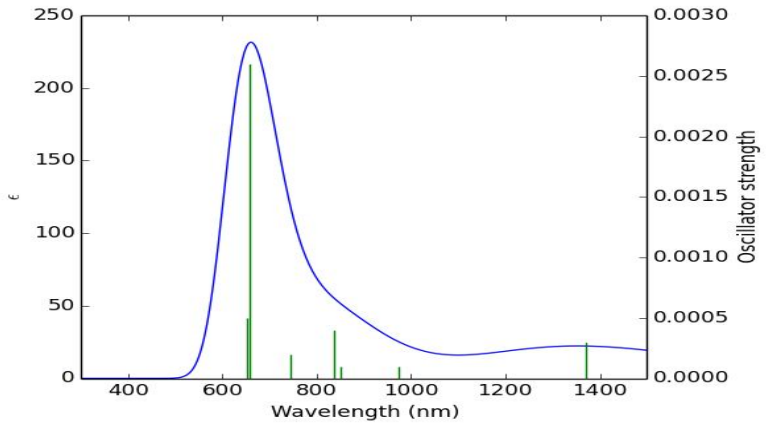

Figure 6: TD-DFT calculated electronic absorption spectra of [$Ge_9(C_6H_5)$].

As observed from **Table 6**, the energies of the probable electronic transitions at gas phase are 0.9056, 1.2731, 1.4567, 1.4830, 1.6665, 1.8815, and 1.9038 eV respectively, similarly the absorption wavelengths are 1369.05, 973.90, 851.12, 836.01, 744.0, 658.95 and 651.24 nm respectively and the corresponding computed oscillator strengths are 0.0003, 0.0001, 0.0001, 0.0004, 0.0002, 0.0026, and 0.0005 respectively. Oscillator strength is expressed by the strength of the transition of the nanocluster from HOMO-LUMO. In UV-vis spectroscopy, it can be experimentally measured by integrating the molar extinction coefficient due to a particular transition. The higher the oscillator strength , the higher the potential of the material to act as light absorber or emitter. The oscillator strength vary in the range of 0-1, where f =1 corresponds to allowed transitions and f =0 to be the forbidden transitions. In the nine-atom germanium-phenyl[$Ge_9(C_6H_5)$] nanocluster, the singlet excited states with forbidden transition or dark singlet appear at f =0. From **Figure 6,** a minor prominent absorption peak appears at 1.905 eV with f =0.0005 and correspond to transitions from HOMO-4-LUMO. In the electronic transition spectra cut-off wavelength is the most

important parameter. The oscillator strength reveals that the higher the oscillator strength stronger is the intensity of the spectrum, in the observed UV spectrum the only maximum peak is found to be with higher intensity having maximum wavelength of 658.9 nm and an approximate oscillator strength of about 0.0026. This maximum wavelength usually represents HOMO-LUMO transition with a higher yield contribution. In some other cases, the first maximum may represent $HOMO - LUMO + n$ or $HOMO - n - LUMO$ transitions. The time-dependent density functional theory calculations at CAM-B3LYP/LANL2DZ level shows that the optical absorption are all within the wavelength range proximity of visible spectra of about 400-800 nm. This predicted emission spectra of germanium-phenyl[$Ge_9(C_6H_5)$] is located in the red visible light region, wavelength(658.9 nm) and energy(1.882 eV) with maximum wavelength at about 1369 nm and 0.9056 eV energy. Therefore if this nanomaterials is to be used in optoelectronics, it will be potentially suitable for visible device applications.

Table 7: Absorption wavelength, excitation energies and oscillator strength computed at CAM- B3LYP/LANL2DZ basis set

S/N	Excitation Energies (eV)	Absorption Wavelength/nm	Orbital Involved	Oscillator Strength, f)	Major contribution
1	0.9056	1369.05	Homo-Lumo	0.0003	0.96
2	1.1576	1071.01	Homo-1-Lumo	0.0000	0.9578
3	1.2731	973.90	Homo-Lumo	0.0001	0.986
4	1.4525	853.57	Homo-1-Lumo+1	0.0000	0.64027
			Homo-Lumo		0.2913
5	1.4567	851.12	Homo-1-Lumo	0.0001	0.54800
			Homo-2-Lumo		0.44738
			Homo-1-Lumo+1		0.35256
6	1.4830	836.01	Homo-2-Lumo	0.0004	0.83243
			Homo-Lumo+1		0.33666
7	1.6665	744.0	Homo-6-Lumo	0.0002	0.26649
			Homo-5-Lumo		0.35802
			Homo-3-Lumo		0.84306
8	1.7755	698.31	Homo-5-Lumo	0.0000	0.84462
9	1.8815	658.95	Homo-1-Lumo	0.0026	0.39692
			Homo-4-Lumo		0.63280
			Homo-Lumo+1		0.54855
10	1.9038	651.24	Homo-4-Lumo	0.0005	0.63880

All major contributions below 0.2 have been neglected.

Electronic Density of States(DOS)

The density of state is a representation of the number of energy levels in a section along the energy axis of width dE, normalized per unit volume. It is defined as ;

$$N(E) = \frac{1}{4\pi^3}\int \delta\left(E - E_n(k)\right)dk \quad (1.19)$$

where $E_n(k)$ is the dispersion of the given band and the integral is determined over the Brillouin zone. For a semiconductor like germanium, this result can be apply to electrons in the conduction band and holes in the valence band. Density of state function is important in the electronic process particularly in transport phenomena. Gauss Sum 3.0 package was used to plot the DOS spectrum and to calculate the HOMO-LUMO gap of the nanostructure. This DOS shows the possible energy flow from occupied(green) to the virtual(red) orbitals. The density of state for the nine-atom germanium-phenyl nanostructure is shown in **Figure 7**. It represent the localization of charges in the conduction band and in the valence band along [$Ge_9(C_6H_5)$] nanocluster system. Typically, each energy level is convoluted

with a Gaussian curve of unit height and a given full width at half maximum where there are many energy levels close together the curves overlap and the spectrum has a peak.

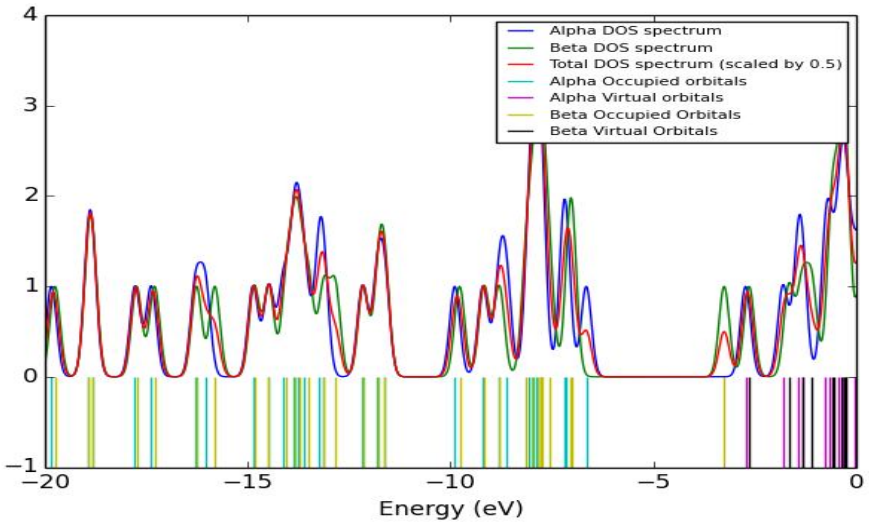

Figure 7: Density of state of germanium-phenyl[$Ge_9(C_6H_5)$] .

The density of state clearly exhibits the possible energy flow from occupied(green color) to the virtual(purple) states. The DOS spectrum shows more peaks in occupied orbital than virtual orbital. It can be found that the highly peaked DOS are observed for the occupied molecular orbitals with many maximum peaks and several subpeaks that represent the localization of charges. The virtual molecular orbital has very few maximum peaks and minimum subpeaks, indicating low charge localization in this region. The HOMO and LUMO are both spread over the entire nanostructure having contributions from the nine-atom Ge atoms and the phenyl elements with the charge density higher in the occupied molecular orbitals than in the virtual orbitals. This also indicates that the HOMO is electron rich site and LUMO is electron poor site. The different maximum peaks, minimum peaks and subpeaks occur at different energy intervals due to bonding of Ge atoms and the phenyl elements in the [$Ge_9(C_6H_5)$] nanocluster. Bakkiyarai *et al*,(2017) reports that a positive value for the DOS show bonding interaction, a negative value shows antibonding and zero value correspond to non-bonding interaction.

Looking at the total DOS, it is also observed that there are the presence of narrow pseudogap with width of 0.6eV located at 0.3 eV above the energy axis, a characteristic feature of quasicrystals having crystalline nature. The pseudogaps arise from the strong hybridization between germanium 3d states and carbon $2S^2$ and $2p^2$ states. Also observed is the large degree of overlap along a wide energy interval indicating that covalent bonding is the dominant type of bonding in the nanostructure.

CONCLUSION

The molecular properties of nine-atom germanium-phenyl nanocluster have been investigated at DFT/B3LYP method with LANL2DZ basis set. The optimized geometry, vibrational frequencies, thermodynamic parameters and density of state of the nanocluster have been calculated. Further, TD-DFT calculations were performed to obtain the optical properties of the structure. The calculated results involving the excitation energies, oscillator strength, f and wavelength were carried out. Typically, the maximum absorption wavelength(λ_{max}) corresponds in UV spectrum to an intense maximum peak at 658.8 nm with oscillator strength $(f = 0.0026)$ in the gas phase. The density of state clearly exhibit the possible energy flow from occupied to the virtual states. The spectroscopic and computational calculations are believed to contribute to the understanding and evaluation of cluster properties for their potential future applications.

REFERENCES

Allen F.H.(2002). The Cambridge Structural Database: a Quarter of a million Crystals Structures and Using: *Acta Crystallographic section* B,38(3-1).

Atobe J.S., Koyasu K., Nakajima A., Furuse S.(2012). Anion Photoelectron Spectroscopy of Germanium and Tin Clusters Containing a Transition or Lanthanide-Metal Atom, MGe(n)-(n=15-17) and MSn(n)-(n=8-20), (M= Sc-V, Y-Nb and Lu-Ta). *Phys. Chem. Chem. Phys.* 14, pp 9403-9410.

Bakkiyaraj D., Periandy S., Xavier S., Joazaizulfazli J.(2017). Analysis of Vibrational, Electronic and Reactivity Properties of Adenine Using Spectroscopic and Computational Tools. J.

Ebenezer (ed). *Recent Trends in Material Science and Applications*, Springer Proceedings in Physics, 189, pp 599-627.

Elmali A., Kabak M., Kavlakoglu E., Elerman Y., Durlu T.N.(1999). Tautomeric Properties, Conformations and Structure of N-(2-Hydroxy-5-Chlorophenyl) Salicylaldimine. *Journal of Molecular Structure*, 510, pp 207-214.

Frisch M. J.; Trucks, G. W.; Schlegel, H. B.; Scuseria, G. E.; Robb, M. A.; Cheeseman, J. R.; Scalmani, G.; Barone, V.; Mennucci, B.; Petersson, G. A.; Nakatsuji, H.; Caricato, M.; Li, X.; Hratchian, H. P.; Izmaylov, A. F.; Bloino, J.; Zheng, G.; Sonnenberg, J. L.; Hada, M.; Ehara, M.; Toyota, K.; Fukuda, R.; Hasegawa, J.; Ishida, M.; Nakajima, T.; Honda, Y.; Kitao, O.; Nakai, H.; Vreven, T.; J. A. Montgomery, J.; Peralta, J. E.; Ogliaro, F.; Bearpark, M.; Heyd, J. J.; Brothers, E.; Kudin, K. N.; Staroverov, V. N.; Kobayashi, R.; Normand, J.; Raghavachari, K.; Rendell, A.; Burant, J. C.; Iyengar, S. S.; Tomasi, J.; Cossi, M.; Rega, N.; Millam, J. M.; Klene, M.; Knox, J. E.; Cross, J. B.; Bakken, V.; Adamo, C.; Jaramillo, J.; Gomperts, R.; Stratmann, R. E.; Yazyev, O.; Austin A. J.; Cammi, R.; Pomelli, C.; Ochterski, J. W.; Martin, R. L.; Morokuma, K.; Zakrzewski, V. G.; Voth, G. A.; Salvador, P.; Dannenberg, J.J.; Dapprich, S.; Daniels, A. D.; Farkas, O.; Foresman, J. B.; Ortiz, J. V.; Cioslowski, J.; Fox, D. J. In *Gaussian 09*; Gaussian, Inc.: Wallingford CT, **2009**.

Goswami S., Sushmita S., Yadav R.K.(2015). Structural, Electronic and Vibrational Properties of $Ge_xC_Y\,(x+y=2-5)$ Nanocluster: A B3LYP-DFT Study. *Physica E*, 74, pp 175-192, Elsevier.

Hansen D.F., Zhou B. and Goicoechea J.M.(2012). Further Studies into the Reactivity and Coordination Chemistry of $Ge_9]^{4-}$ Zintl ions. The Indium Containing Anions$[In(Ge_9)_2]^{5-}$, $[Ge_9In(C_6H_5)]^{4-}$, $Ge_9[[In(C_6H_5)_3]_2]^{4-}$. *Journal*

of Organometallic Chemistry, pp53-61

Hay P.J. and Wadt W. R. (1985). *Journal of Chemical Physics*, 82(270).

Herrera C, and Seminario J.M.(2007). Study of Nanostructure Silicon-phenyl nanocluster towards single molecule sensing. *International Journal of High Speed Electronics and Systems.* 17(2), pp327-338, World Scientific.

Hull M.W., and Sevov S. C.(2009). Functionalization of Nine-Atom Deltahedral Zintl Ions with Organic Substituent: Detailed Studies of the Reactions. *Journal of American Chemical Society*, 131, pp 9026-9037.

Jensen F.(2007). Introduction to Computational Chemistry, 2nd Edition, John Wiley& Sons, UK

Kagan C.R., Mitzi D.B., Dimitrakopoulous C.D.(1999). Organic-Inorganic Hybrid Materials as Semiconducting channels in thin film Field-Effect-Transistors. *Science,* Vol.286, pp 945-947.

Kapil D., Ravi T., Bandyopadhyay D.(2012).Electronic Structure and Stabilities of Ni-doped Germanium Nanoclusters: a Density Functional Modeling Study, *Journal of Molecular Model*.

Leach A. R.(2007). Molecular Modeling: Principles and Applications. Addison Wesley, Longman Limited, Harlow.

O'Boyle N.M., Tenderholt A.L., Langner K.M.(2008). A Library for Package independent Computational Chemistry Algorithms. *Journal Computational Chemistry*, 29, pp 839-845.

Pancharatna D.P. and Hoffmann R.(2006). Theoretical Studies on Doubly and Triply linked Polymers of Ge_9 Clusters. *Inorganica Chimica Acta*, 359, pp 3776-3784, Elsevier

Pecher J., Gerson M., Michael D., Tonner R.(2017). Site-Specific Reactivity of Ethylene at Distorted Dangling-Bond Configuration on Si(001). *Chem.Phys.Chem*, 18, pp 357-365.

Raj P.S., Periandy S., Xavier S. and Mohamed I.A.(2017). Molecular Structure, Vibrational Spectra, HOMO, LUMO and NMR Studies of Methylphenylcyclopropeno ne based on DFT. J. Ebenezer (ed). *Recent Trends in Material Science and Applications*, Springer Proceedings in Physics, 189, pp 655-683.

Reena D., Prabhakar S., Rajiv D., Rajendra P.(2013). A DFT Study of the Conformational Behavior of N'"- [(1-(2-hydroxy-5-methylphenyl) ethylidene] Carbohydrazide. *International Journal of Scientific & Engineering Research*, 4(11) pp1337-1342.

Saikia N., Maximihan S., Ravindra P.(2016). Stability and Electronic Properties of 2D Nanomaterials Conjugated with Pyrazinamide Chemotherapeutic: A First Principles Cluster Study. *The Journal of Physical Chemistry* C.

Shim I., Sai Baba M., Gingerich K.A.(1998). Electronic Structure and Thermodynamic Calculations and Knudsen Effusion mass Spectrometric Measurement. *Journal Physical Chemistry* A, 102, pp 10763-10767.

Sholl D.S., and Steckel (2009). Density Functional Theory: A Practical Introduction, John Wiley & Sons Inc.

Suna P., Hota P., Misra P.K.(2016). Experimental and Theoretical Studies on the Structure, Electronic and Vibrational Spectra of 0/p-hydroxybenzylidenes. *Indian Journal of Chemistry*, 55A , pp1192-1201.

Sun Z. M., Zhao Y. F., Li J., Wang L.S.(2009). Diversity of Functionalized Germanium Zintl Clusters: Syntheses and Theoretical Studies of $[Ge_9PdPPh_3]^{3-}$ and $[Ni@(Ge_9PdPPh_3)]^{2-}$.*Journal of Cluster Science*, 20, pp 602-609, Springer.

Wielgus P., Szczepan R.,Majumdar D., Julia S., Jerzy L.(2008). Theoretical Studies on the Bonding and Thermodynamic Properties of Ge_nSi_m (m+n=5) Clusters. The precursors of Germanium/Silicon Nanomaterials. *The Journal*

of Chemical Physics, 128,
pp 144305-1/144305-10.